

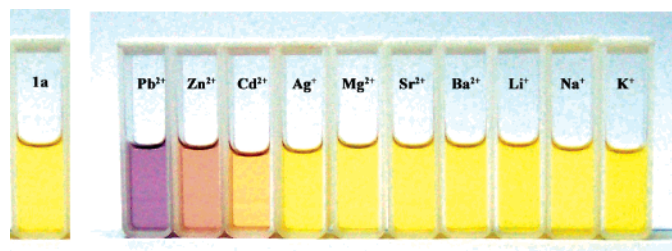
Highly Selective Colorimetric and Electrochemical Pb²⁺ Detection Based on TTF- π -Pyridine Derivatives

Hai Xue,^{†,‡} Xin-Jing Tang,[†] Li-Zhu Wu,^{*,†} Li-Ping Zhang,[†] and Chen-Ho Tung^{*,†}

Technical Institute of Physics and Chemistry and The Graduate School of Chinese Academy of Sciences, Chinese Academy of Sciences, Beijing 100101, China

lzwu@mail.ipc.ac.cn; chtung@mail.ipc.ac.cn

Received June 1, 2005



The pyridineethenyl-substituted tetrathiafulvalene (TTF) compounds, 4-(4-pyridineethenyl)tetrathiafulvalene (**1a**) and 4,4'(5')-[bis-(4-pyridineethenyl)]tetrathiafulvalene (**2a**) together with the styryl-substituted TTF compounds, 4-styryltetrathiafulvalene (**1b**) and 4,4'(5')-bis-styryltetrathiafulvalene (**2b**), have been designed and synthesized. All these compounds exhibit strong absorption bands in the range of 370 to 550 nm, which are assigned to the intramolecular charge-transfer transition from the HOMO in TTF to the LUMO in the pyridyl or phenyl group. Compared to compounds **1b** and **2b**, the pyridineethenyl-substituted TTF compounds **1a** and **2a** show remarkable sensing and coordinating properties to Pb²⁺. With the addition of micromolar concentrations of Pb²⁺ to the solution, **1a** or **2a** displays dramatic changes in the UV-vis absorption spectrum, ¹H NMR spectrum, and redox property.

Introduction

Among heavy metals, lead is the most commonly encountered toxic pollutant in the environment as a result of its current and previous use in batteries, gasoline, and paints.^{1,2} Lead is known to cause health problems, such as digestive, neurological, cardiac, and mental troubles. In particular, it is dangerous for children, causing mental retardation. Therefore, the development of methods for measuring the level of this detrimental ion in the environment with high sensitivity and selectivity is highly desirable. Currently, amounts of lead are mainly determined using atomic absorption or emission spectrometers.^{1,2} Herein, we report two tetrathiafulvalene (TTF) based compounds specific for detection of Pb²⁺ with high sensitivity by monitoring the changes both in color and in electrochemistry.

Supramolecular systems containing both redox active TTF functionality^{3–15} and a host unit capable of cation binding have attracted considerable attention during past decades because the complexation of the host with an ionic guest may induce large changes in the redox

* Corresponding authors. Phone: +86-10-64855186; fax: (0086)-10-64879375.

[†] Technical Institute of Physics and Chemistry.

[‡] The Graduate School of Chinese Academy of Sciences.

(1) Métivier, R.; Leray, I.; Valeur, B. *Chem. Commun.* **2003**, 996–997.

(2) Battistuzzi, G.; Borsari, M.; Menabue, L.; Saladini, M.; Sola, M. *Inorg. Chem.* **1996**, *35*, 4239–4247.

(3) (a) Garin, J. *Adv. Heterocycl. Chem.* **1995**, *62*, 249–304. (b) Boulas, P. L.; Gómez-Kaifer, M.; Echegoyen, L. *Angew. Chem., Int. Ed.* **1998**, *37*, 216–247 and *Angew. Chem.* **1998**, *110*, 226–258. (c) Schukat, G.; Fanghänel, E. *Sulfur Rep.* **1996**, *18*, 1–294.

(4) (a) Bryce, M. R. *J. Mater. Chem.* **2000**, *10*, 589–598. (b) Bryce, M. R. *Adv. Mater.* **1999**, *11*, 11–23.

(5) (a) Segura, J. L.; Martín, N. *Angew. Chem., Int. Ed.* **2001**, *40*, 1372–1409. (b) Jeppesen, J.; Becher, J. *Eur. J. Org. Chem.* **2003**, 3245–3266. (c) Nielsen, K.; Jeppesen, J.; Levillain, E.; Becher, J. *Angew. Chem., Int. Ed.* **2003**, *42*, 187–191.

(6) (a) Jørgensen, T.; Hansen, T. K.; Becher, J. *Chem. Soc. Rev.* **1994**, *23*, 41–51. (b) Nielsen, M. B.; Lomholt, C.; Becher, J. *Chem. Soc. Rev.* **2000**, *29*, 153–164.

(7) (a) Díaz, M. C.; Illescas, B. M.; Seoane, C.; Martín, N. *J. Org. Chem.* **2004**, *69*, 4492–4499. (b) Otero, M.; Herranz, M. Á.; Seoane, C.; Martín, N.; Garin, J.; Orduna, J.; Alcalá, R.; Villacampa, B. *Tetrahedron* **2002**, *58*, 7463–7475 (c) Herranz, M. A.; Martín, N.; Sánchez, L.; Garin, J.; Orduna, J.; Villacampa, B.; Villacampa, B.; Sánchez, C. *Tetrahedron* **1998**, *54*, 11651–11658 (d) González, M.; Segura, J. L.; Seoane, C.; Martín, N.; Garin, J.; Orduna, J.; Alcalá, R.; Villacampa, B.; Hernández, V.; López-Navarrete, J. T. *J. Org. Chem.* **2001**, *66*, 8872–8882.

properties in the systems.^{5–15} The TTF moiety can undergo two successive reversible 1e oxidations to TTF^{•+} and TTF²⁺ at E^1_{ox} and E^2_{ox} , respectively.^{8a,8b,12} Upon complexation of the host unit with metal cations in a TTF–receptor system, the proximity between the ion and the TTF moiety will alter the oxidability of the TTF framework and make its E^1_{ox} positive shift. However, the E^2_{ox} value generally remains unchanged upon addition of metal ions since when reaching E^2_{ox} the increased repulsive electrostatic interactions between TTF²⁺ and the guest cation would result in the expulsion of the metal ion from the host. The E^1_{ox} shift upon metal complexation has been extensively used for sensing purposes. For example, incorporation of the TTF unit into a macrocyclic recognition motif has allowed the electrochemical recognition of various metal cations.^{3,5,8,9,12} Becher and co-workers investigated the TTF–crown ether and TTF–thiocrown ether derivatives as well as a TTF–cryptand derivative for their potential use as electroactive cation sensors.^{8b–8d} A shift in the value of E^1_{ox} to a more anodic potential was observed upon addition of metal ions (Li⁺, Na⁺, K⁺, Ag⁺, Ba²⁺) to a solution of a variety of TTF–crown molecules. Several TTF–crown derivatives exhibited good selectivity for Ag⁺ ions:^{8b,8e,8f,12a} the addition of a controlled amount of silver triflate to the solution of such TTF–crowns resulted in a positive shift of E^1_{ox} , and no shift of E^1_{ox} was observed upon addition of a wide variety of Group 1 and 2 or other transition metal ions. Later, Sallé and Becher reported

that the macrocyclic systems containing a bis(pyrrolo)-tetrathiafulvalene moiety and polyether subunits displayed high binding affinities for Pb²⁺ and Ba²⁺ cations.^{9a} ¹H NMR and UV–vis spectroscopy showed that metallic cations were complexed within the macrocyclic receptor. Binding constants in the range of 10⁵ to 10⁶ M^{−1} in a 1:1 mixture solvent of CH₃CN and CH₂Cl₂ were obtained from titration studies, which correspond to the highest binding strength reported so far for a TTF-based cation receptor. Echegoyen and co-workers¹³ synthesized bis-thioctic ester derivatives of TTF unit annelated with crown ethers and assembled them into monolayers on gold electrodes. The prepared electrochemically active SAMs show promise as potential thin-film sensors for metal ions. Bryce and co-workers¹⁴ reported crown-annelated TTF derivatives containing a single alkyl chain terminated with a thiol group. The monolayers on gold or platinum surfaces could electrochemically recognize metal cations such as Na⁺, Ba²⁺, and Ag⁺. Very recently, Sallé and co-workers¹⁵ reported the preparation of a modified surface with a TTF based redox-switchable ligand, which exhibits good specificity for Pb²⁺ over other cations and is able to bind (TTF⁰ state) or expel the metal cation upon oxidation (TTF²⁺ state).

Although a very large proportion of molecular systems containing the redox-active TTF functionality together with macrocyclic(s) has been investigated, few cation complexation studies have been carried out on the TTF derivatives with noncyclic binding units. On the other hand, the association of a TTF core with pyridine ligands has been investigated to offer a novel perspective on the modulation of architecture and multifunctional molecular materials.^{10,11} It should be pointed out that the TTF derivatives functionalized with pyridine together with their transition metal complexes have been synthesized, aimed to improve the π -d interaction between the conducting and the localization spin systems.¹¹ However, there are few examples taking advantage of TTF as a donor in intramolecular charge-transfer molecules for cation recognition. In the present work, we link pyridyl group(s) with a TTF moiety through double bond bridge(s), as shown in Scheme 1. The pyridyl group(s) acts as the monodentate ligand(s) for metal ions. The π -conjugated double bond was designed as the linkage to optimize the communication between the receptor and the TTF core. As expected, both **1a** and **2a** exhibit dramatic color and electrochemical changes upon exposure to micromolar concentrations of Pb²⁺.

Results and Discussion

Synthesis. Compound **1** (or **2**) was modified by introducing simple pyridyl or phenyl group(s) to a TTF unit linked by π -conjugated double bond(s). As presented in Scheme 1, **1** and **2** were synthesized according to the procedures described in the literature.^{16–18} Treatment of

(8) (a) Hansen, T. K.; Jørgensen, T.; Stein, P. C.; Becher, J. *J. Org. Chem.* **1992**, *57*, 6403–6409. (b) Le Derf, F.; Sallé, M.; Mercier, N.; Becher, J.; Richomme, P.; Gorgues, A.; Orduna, J.; Garin, J. *Eur. J. Org. Chem.* **1998**, 1861–1865. (c) Le Derf, F.; Mazari, M.; Mercier, N.; Levillain, E.; Richomme, P.; Becher, J.; Garin, J.; Orduna, J.; Gorgues, A.; Sallé, M. *Inorg. Chem.* **1999**, *38*, 6096–6100. (d) Le Derf, F.; Mazari, M.; Mercier, N.; Levillain, E.; Richomme, P.; Becher, J.; Garin, J.; Orduna, J.; Gorgues, A.; Sallé, M. *Chem. Commun.* **1999**, 1417–1418. (e) Bryce, M. R.; Batsanov, A. S.; Finn, T.; Hansen, T. K.; Howard, J. A. K.; Kamenjicki, M.; Lednev, I. K.; Asher, S. A. *Chem. Commun.* **2000**, 295–296. (f) Johnston, B.; Goldenberg, L. M.; Bryce, M. R.; Katakay, R. *J. Chem. Soc., Perkin Trans. 2* **2000**, 189–190.

(9) (a) Trippé, G.; Levillain, E.; Le Derf, F.; Gorgues, A.; Sallé, M.; Jeppesen, J. O.; Nielsen, K.; Becher, J. *Org. Lett.* **2002**, *4*, 2461–2464. (b) Le Derf, F.; Mazari, M.; Mercier, N.; Levillain, E.; Trippé, G.; Riou, A.; Richomme, P.; Becher, J.; Garin, J.; Orduna, J.; Gallego-Planas, N.; Gorgues, A.; Sallé, M. *Chem.–Eur. J.* **2001**, *7*, 447–455.

(10) (a) Devic, T.; Avarvai, N.; Batail, P. *Eur. J. Chem.* **2004**, *10*, 3697–3707. (b) Liu, S.-X.; Dolder, S.; Franz, P.; Neels, A.; Stoeckli-Evans, H.; Decurtins, S. *Inorg. Chem.* **2003**, *42*, 4801–4803. (c) Griffiths, J.-P.; Brown, R. J.; Day, P.; Matthews, C. J.; Vital, B.; Wallis, J. D. *Tetrahedron Lett.* **2003**, *44*, 3127–3131. (d) Campagna, S.; Serroni, S.; Puntoriero, F.; Loiseau, F.; DeCola, L.; Kleverlaan, C. J.; Becher, J.; Sørensen, A. P.; Hascoat, P.; Thorup, N. *Chem.–Eur. J.* **2002**, *8*, 4461–4469.

(11) (a) Iwahori, F.; Golhen, S.; Ouahab, L.; Carlier, R.; Sutter, J.-P. *Inorg. Chem.* **2001**, *40*, 6541–6542. (b) Setifi, F.; Ouahab, L.; Golhen, S.; Yoshida, Y.; Saito, G. *Inorg. Chem.* **2003**, *42*, 1791–1793. (c) Ouahab, L.; Iwahori, F.; Golhen, S.; Carlier, R.; Sutter, J.-P. *Synth. Met.* **2003**, *133–134*, 505–507.

(12) (a) Dieing, R.; Morisson, V.; Moore, A. J.; Goldenberg, L. M.; Bryce, M. R.; Raoul, J. M.; Petty, M. C.; Garin, J.; Saviron, M.; Lednev, I. K.; Hester, R. E.; Moore, J. N. *J. Chem. Soc., Perkin Trans. 2* **1996**, 1587–1594. (b) Nielsen, M. B.; Becher, J. *Liebigs Ann.* **1997**, 2177–2187.

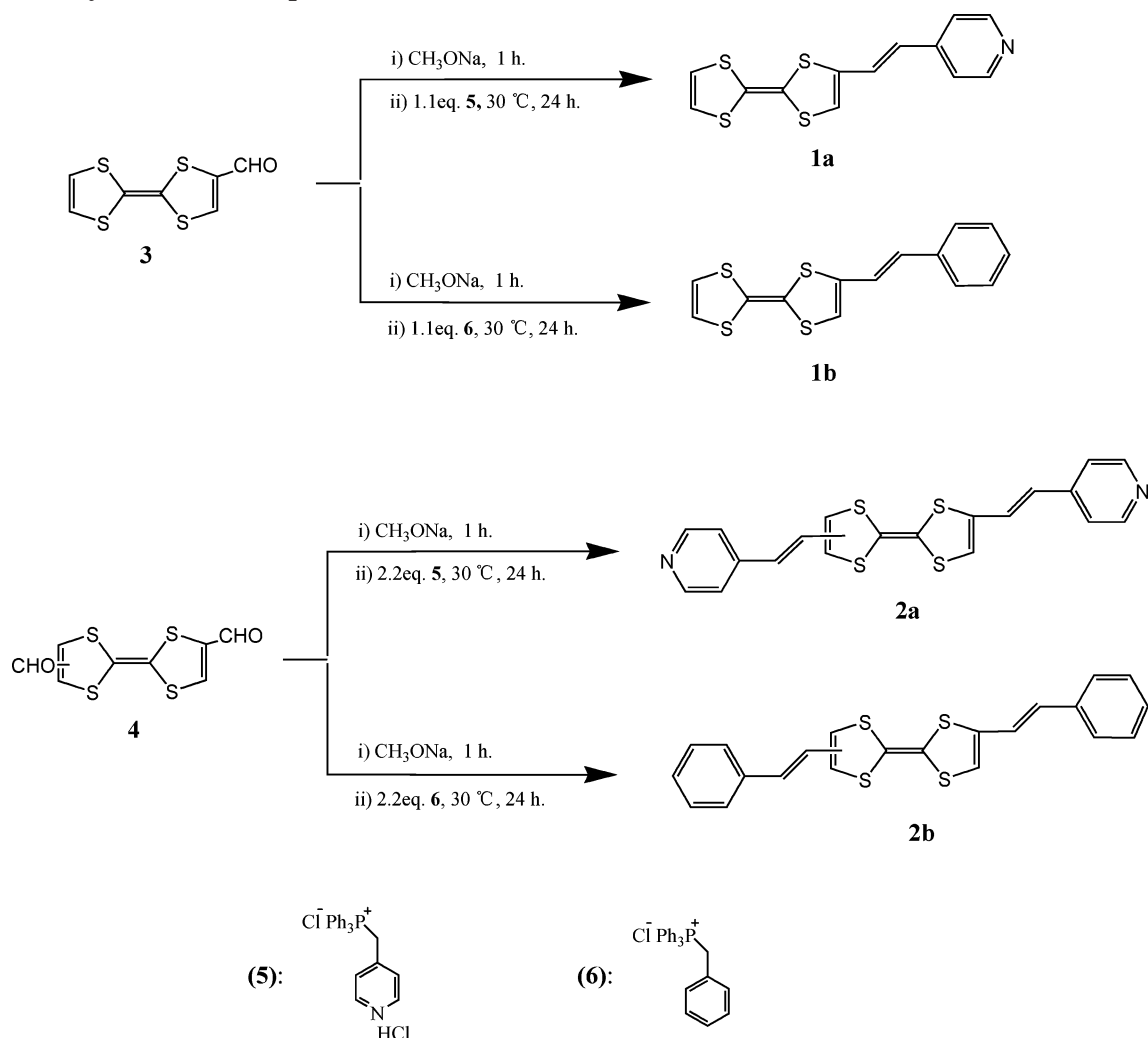
(13) (a) Liu, H. L.; Liu, S.; Echegoyen, L. *Chem. Commun.* **1999**, 1493–1494. (b) Liu, S. G.; Liu, H.; Bandyopadhyay, K.; Gao, Z.; Echegoyen, L. *J. Org. Chem.* **2000**, *65*, 3292–3298.

(14) Moore, A. J.; Goldenberg, L. M.; Bryce, M. R.; Petty, M. C.; Monkman, A. P.; Marenco, C.; Yarwood, J.; Joyce, M. J.; Port, S. N. *Adv. Mater.* **1998**, *10*, 395–398.

(15) (a) Lyskawa, J.; Le Derf, F.; Levillain, E.; Mazari, M.; Sallé, M.; Dubois, L.; Viel, P.; Bureau, C.; Palacin, S. *J. Am. Chem. Soc.* **2004**, *127*, 12194–12195. (b) Trippé, G.; Le Derf, F.; Lyskawa, J.; Mazari, M.; Roncali, J.; Gorgues, A.; Levillain, E.; Sallé, M. *Chem.–Eur. J.* **2004**, *10*, 6497–6509.

(16) Andreu, R.; Malfant, I.; Lacroix, P. G.; Cassoux, P. *Eur. J. Org. Chem.* **2000**, 737–741.

(17) (a) Melby, L. R.; Hartzler, H. D.; Sheppard, W. A. *J. Org. Chem.* **1974**, *39*, 2456–2458. (b) Wudl, F.; Kaplan, M. L.; Hufnagel, E. J.; Southwick, E. W. *J. Org. Chem.* **1974**, *39*, 3608–3609. (c) Garin, J.; Orduna, J.; Unel, S.; Moore, A. J.; Bryce, M. R.; Wegener, S.; Yufit, O. S.; Howard, J. A. K. *Synthesis* **1994**, 489–491.

SCHEME 1. Synthesis of Compounds **1** and **2**

4-monoformyl-tetrathiafulvalene (**3**) or 4,4'(5')-bisformyl-tetrathiafulvalene (**4**) with phosphonium salts **5** and **6** at room temperature afforded corresponding compound **1a** (60%), **1b** (46%), **2a** (29%), and **2b** (40%), respectively. The mild reaction condition by employing CH₃ONa as a base to carry out the Wittig reaction simplified the operations when LDA was used. 4-Monoformyl-tetrathiafulvalene **3** was obtained with a yield of 60% by using *N*-methyl-*N*-phenylformamide as the formylating reagent, as described by Garin and Bryce.^{17c} Preparation of 4,4'(5')-bisformyl-tetrathiafulvalene **4** was achieved by several routes starting from 1,3-dioxolan-2-yl-1,3-dithiole-2-thione followed by a coupling reaction with P(OEt)₃ and hydrolysis.¹⁸ The corresponding phosphonium salts were prepared according to the literature procedure.¹⁹ The yield of compound **1** was much higher than that of **2** may be due to the solubility of 4-monoformyl-tetrathiafulvalene **3** was much better than that of 4,4'(5')-bisformyl-tetrathiafulvalene **4** in THF. The identities of

the compounds were confirmed by ¹H NMR spectroscopy, ¹³C NMR spectroscopy, MS spectrometry, and satisfactory elemental analyses.

Selectively Colorimetric Detection of Pb²⁺. The absorption spectra of **1a**, **2a** and their model compounds **1b**, **2b** as well as the parent TTF in acetonitrile solution were investigated and are shown in Figure 1. All these compounds exhibit intense absorption bands at $\lambda < 370$ nm with extinction coefficients on the order of 10⁴ dm³ mol⁻¹ cm⁻¹. In addition, **1a**, **2a**, **1b**, and **2b** show a moderately intense absorption band in the region of 370 to 550 nm, while such a band is absent for the parent TTF. The absorption properties were found to follow Beer's law below concentrations of 1 \times 10⁻⁴ mol dm⁻³, suggesting the absence of significant complex aggregation. It has been established that for electron acceptor-TTF compounds, the HOMO is located on the TTF moiety, whereas the LUMO is located on the electron acceptor fragment.¹⁶ Thus, the band in 370 to 550 nm is ascribed to the intramolecular charge-transfer transition (CT) from the HOMO in TTF to the LUMO in the pyridyl (for **1a** and **2a**) or phenyl group (for **1a** and **2b**), while the bands at $\lambda < 370$ nm are assigned to the local transition in the TTF moiety. Compared with **1b** and **2b**,

(18) (a) Andreu, R.; Garin, J.; Orduna, J.; Coussaeanu, J.; Gorgues, A.; Morisson, V.; Nozdryn, T.; Becher, J.; Clausen, R. P.; Bryce, M. R.; Skabara, P. J.; Dehaen, W. *Tetrahedron Lett.* **1994**, *35* (49), 9243–9246. (b) Clausen, R. P.; Becher, J. *Tetrahedron* **1996**, *52* (9), 3171–3188.

(19) Baker, B. R.; Doll, M. H. *J. Med. Chem.* **1971**, *14*, 793–799.

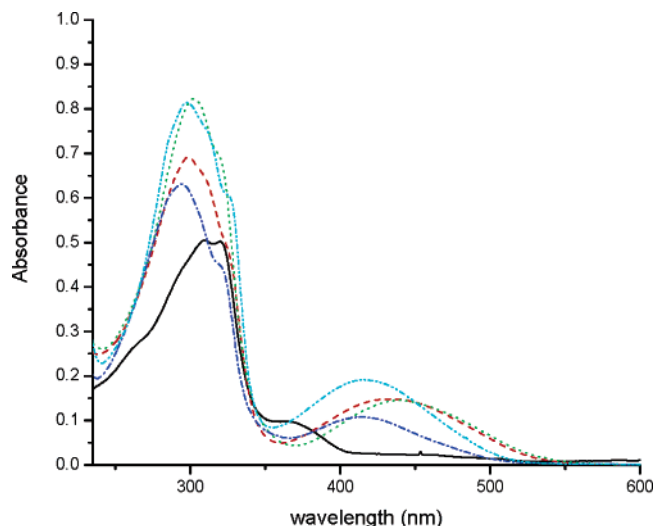


FIGURE 1. Absorption spectra of **1a** (---), **2a** (.....), **1b** (-.-.-), **2b** (----), and the parent TTF (—) in CH_3CN solution ($10^{-5} \text{ mol dm}^{-3}$) at room temperature.

the CT bands for **1a** and **2a** are red-shifted ca. 25 nm. This observation evidently arises from the stronger electron-accepting ability of the pyridyl group than the phenyl group.

The pyridyl group(s) in **1a** and **2a** can serve as monodentate ligands, and the interaction between the pyridyl and the metal cations, particularly Pb^{2+} , leads to dramatic changes in the absorption spectra of **1a** and **2a**. Figure 2 presents changes in the UV-vis spectra of **1a** and **2a** upon addition of Pb^{2+} , available as the perchlorate salt, to the solutions of **1a** and **2a** in acetonitrile (in the presence of $0.1 \text{ mol dm}^{-3} n\text{Bu}_4\text{NPF}_6$). Both the CT bands and the local transition bands are red-shifted. The local absorption band with λ_{max} at 301 nm and the CT transition band with λ_{max} at 440 nm of **1a** decreased monotonically throughout the addition, and the new bands with λ_{max} at 330 and 555 nm appeared and concomitantly grew in with increasing Pb^{2+} concentration. Well-defined isosbestic points at 485, 388, 323, and 248 nm are clearly observed, indicating the presence of only two absorption species in the solution: the free **1a** and the complex **1a**· Pb^{2+} . At the end of the titration, the solution color changes from yellow to deep purple. The CT band is red-shifted ca. 115 nm, which is, to the best of our knowledge, the largest bathochromic shift for TTF derivatives so far reported upon exposing to external cation stimulus. Similar results were observed upon addition of Pb^{2+} to the solution of **2a** in acetonitrile. The red-shifts in the CT band arise from the complexation of the cation with the pyridyl group(s) in **1a** and **2a**, which increases the electron-accepting ability of the pyridyl, hence decreasing the LUMO of the molecules. The red-shifts in the local transition bands suggest that the complexation between pyridyl ligand and Pb^{2+} also influences the orbital energy level of the TTF moiety. Indeed, control experiments with **1b** and **2b** showed that no such changes in the absorption spectrum could be observed upon addition of the cation under identical conditions. The inserts in Figure 2 show the plots of A versus $[\text{Pb}^{2+}]$, where A refers to the absorbance at 555 nm for **1a** and that at 540 nm for **2a** in the presence of Pb^{2+} . Analysis of the plots by using the Hildebr and

Benesi equation (see eq 1)²⁰ reveals that the complexation of the ion to the pyridyl is in a ratio of 1:2 ($\text{Pb}^{2+}/\text{pyridyl}$). Thus, the stoichiometry for the **1a** complex is 2:1 (**1a**/ Pb^{2+}), while that for the **2a** complex is 1:1 (**2a**/ Pb^{2+}). The binding constants ($\log K_b$) determined from such plots are 5.42 and 5.57 for **1a** and **2a**, respectively, which are comparable with the largest binding constants reported so far for TTF based ligands.

The pyridyl group in **1a** and **2a** can also complex with Zn^{2+} , Cd^{2+} , and Ag^+ , available as the perchlorate salts, as reflected in the absorption spectral changes of the **1a** and **2a** solutions. Figure 3 shows the changes in the absorption spectrum of **1a** in acetonitrile upon addition of $\text{Zn}(\text{ClO}_4)_2$ and $\text{Cd}(\text{ClO}_4)_2$, respectively. It is apparent that the spectral changes are much less significant as compared with that of Pb^{2+} . The Zn^{2+} - and Cd^{2+} -induced red-shifts of the CT bands in the absorption spectra of **1a** (ca. 14 and 8 nm, respectively) are evidently smaller than the case of Pb^{2+} (ca. 115 nm). At the same time, the intensity of the CT band for **1a**· Zn^{2+} or **1a**· Cd^{2+} complexes is considerably weaker than that of **1a**· Pb^{2+} . Obviously, complexation between the pyridyl in **1a** with Zn^{2+} and Cd^{2+} also leads to the increase in the electron-accepting ability of the pyridyl, but the increase extents are much smaller than that of Pb^{2+} .

Unlike TTF-crown ether systems,^{3,5,8,9,12} alkali and alkaline earth metal cations do not affect the absorption spectra of **1a** and **2a**. Thus, **1a** and **2a** can specifically signal Pb^{2+} even in the presence of such metal cations with high concentrations. Figure 4 presents the absorbance at wavelength of 555 nm (the λ_{max} for **1a**· Pb^{2+} complex) for **1a** in the presence of various metal cations in an acetonitrile solution. Evidently, **1a** can specifically respond to Pb^{2+} , and other cations do not interfere with the detection.

¹H NMR Changes of 1a and 2a upon Addition of Pb^{2+} . The specific sensing properties of **1a** and **2a** toward Pb^{2+} were further confirmed by ¹H NMR titration experiments. Figure 5 shows the ¹H NMR spectra of **1a** in CD_3COCD_3 in the presence of various amounts of Pb^{2+} . Comparison of the ¹H NMR spectra of **1a** in the presence and absence of Pb^{2+} reveals that the chemical shifts of the resonances associated with the pyridyl protons and the ethenyl protons show significant changes upon complexation with Pb^{2+} . The signals of the protons in the TTF moiety are also shifted downfield, but the changes are smaller as compared with those for pyridyl protons. These observations suggest that Pb^{2+} is complexed with pyridyl and that the whole molecule of **1a** is a conjugation system. Similar ¹H NMR spectral changes were observed for **2a** upon addition of Pb^{2+} . In contrast, addition of Pb^{2+} to the solution of **1b** or **2b** under identical conditions did not cause any changes in their ¹H NMR spectra. It is important to note that the response of the ¹H NMR spectra of **1a** and **2a** for Pb^{2+} is specific. Alkali and alkaline earth metal cations such as Li^+ , Na^+ , K^+ , Mg^{2+} , Sr^{2+} , and Ba^{2+} do not interfere with the detection of Pb^{2+} .

Pb^{2+} -Induced Redox Potential Changes of 1a and 2a. As mentioned previously, the electrochemical property of TTF is unique. This moiety can be oxidized to its radical cation ($\text{TTF}^{\cdot+}$) and dication (TTF^{2+}) sequentially

(20) Connors, K. A. *Binding Constant: the Measurement of Molecular Complex Stability*; John Wiley & Sons: New York, 1987.

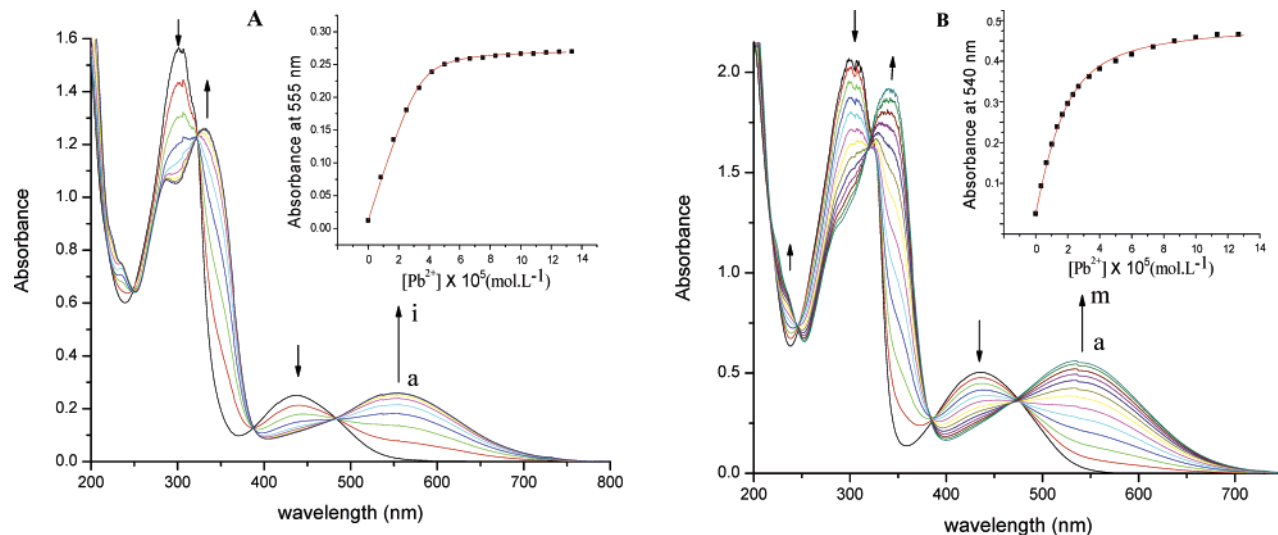


FIGURE 2. (A) Absorption spectra of **1a** ($5.2 \times 10^{-5} \text{ mol dm}^{-3}$) in CH_3CN with $0.1 \text{ mol dm}^{-3} n\text{Bu}_4\text{NPF}_6$ as a function of $\text{Pb}(\text{ClO}_4)_2$ concentration; $[\text{Pb}^{2+}]$: a \rightarrow i, $0 \rightarrow 6.6 \times 10^{-5} \text{ mol dm}^{-3}$. (B) Absorption spectra of **2a** ($6.0 \times 10^{-5} \text{ mol dm}^{-3}$) in CH_3CN with $0.1 \text{ mol dm}^{-3} n\text{Bu}_4\text{NPF}_6$ as a function of $\text{Pb}(\text{ClO}_4)_2$ concentration; $[\text{Pb}^{2+}]$: a \rightarrow m, $0 \rightarrow 6.1 \times 10^{-5} \text{ mol dm}^{-3}$. The inserts show the plots of absorbance at 555 nm for **1a** and that at 540 nm for **2a** against $[\text{Pb}^{2+}]$.

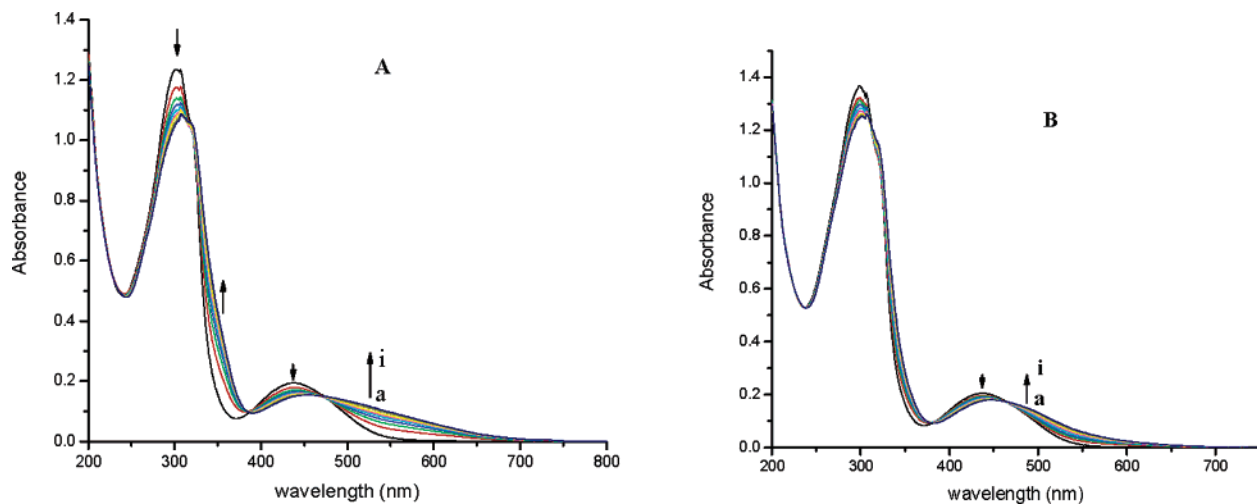


FIGURE 3. Absorption spectra of **1a** ($4.9 \times 10^{-5} \text{ mol dm}^{-3}$) in CH_3CN with $0.1 \text{ mol dm}^{-3} n\text{Bu}_4\text{NPF}_6$ as a function of concentration of (A) $\text{Zn}(\text{ClO}_4)_2$ ($[\text{Zn}^{2+}]$: a \rightarrow i, $0 \rightarrow 6.2 \times 10^{-5} \text{ mol dm}^{-3}$) and (B) $\text{Cd}(\text{ClO}_4)_2$ ($[\text{Cd}^{2+}]$: a \rightarrow i, $0 \rightarrow 5.3 \times 10^{-5} \text{ mol dm}^{-3}$).

and reversibly at low potentials. Table 1 shows the oxidative potentials of **1a** and **2a**, their models **1b** and **2b**, and the parent TTF as well. All these compounds exhibit two reversible one-electron oxidation waves, derived from the oxidation of TTF to $\text{TTF}^{\cdot+}$ and TTF^{2+} , respectively. Both E_{ox}^1 and E_{ox}^2 of **1a** occur at more positive potentials than those of **1b**. Similar results were observed for **2a** and **2b**. The more electron-withdrawing ability of pyridyl group in **1a** and **2a** relative to the phenyl group in **1b** and **2b** makes the oxidation of the TTF core more difficult. The bis-pyridyl and bis-phenyl compounds **2a** and **2b** show much higher oxidation potentials as compared with those of their corresponding monosubstituted compounds **1a** and **1b**, suggesting that introduction of an additional electron-withdrawing group to the molecules leads to more difficulty in oxidation of the TTF moiety.

Complexation of pyridyl group(s) in **1a** and **2a** with Pb^{2+} causes significant changes in the TTF oxidation potentials. Figure 6 presents the cyclic voltammetry (CV)

of **1a** and **2a** as a function of added Pb^{2+} concentrations. Progressive addition of Pb^{2+} (as $\text{Pb}(\text{ClO}_4)_2$) to the solution of **2a** in acetonitrile results in the positive shifts of its E_{ox}^1 and E_{ox}^2 (Figure 6B). In the presence of excess of Pb^{2+} , the first anodic peak potential E_{ox}^1 shifts from 578 to 695 mV and the second E_{ox}^2 from 945 to 980 mV. Thus, ΔE_{ox}^1 and ΔE_{ox}^2 are ca. 117 and 35 mV, respectively. Similar shifts of E_{ox}^1 and E_{ox}^2 for **1a** were observed upon addition of Pb^{2+} (Figure 6A). Evidently, complexation of Pb^{2+} enhances the electron-accepting ability of the pyridyl group(s), which in turn causes the decrease in electron density in the TTF core. This proposal was further supported by the observation that the addition of Pb^{2+} to the solution of **1b** and **2b** did not cause any change in the oxidation potentials of their TTF moiety. It is noteworthy that the second oxidation potential of the TTF moiety in **1a** and **2a** is also altered upon addition Pb^{2+} . This observation is in contrast to the case for TTF-macroyclic systems reported in the literature,^{9,15} in which the second oxidation potential of the TTF moiety

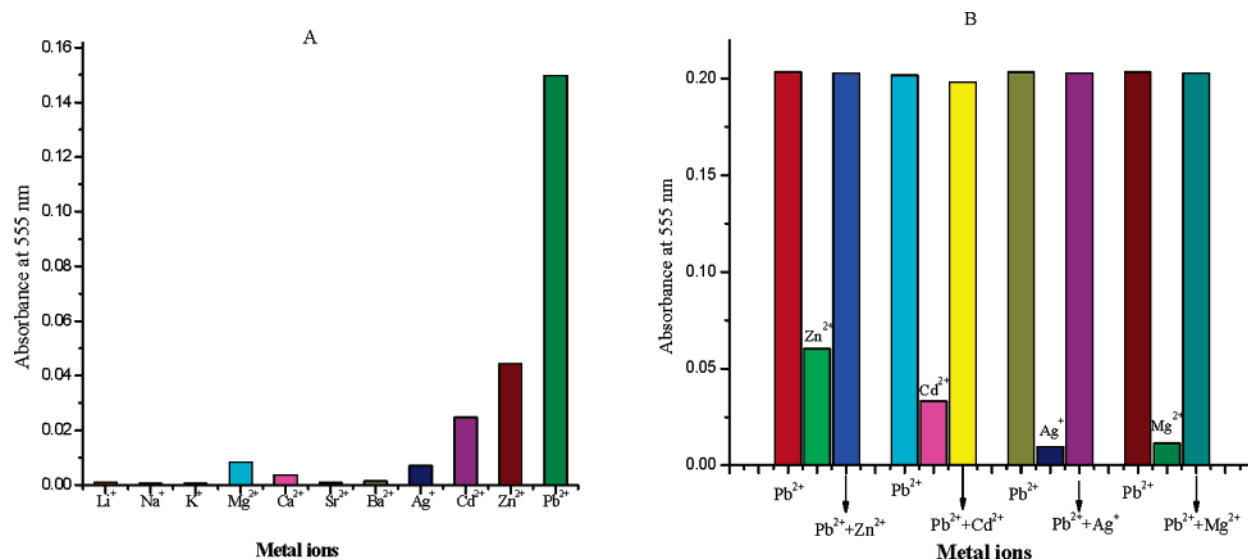


FIGURE 4. Selective response of Pb²⁺ over other metal cations based on the absorbance at 555 nm for **1a** (3.1×10^{-5} mol dm⁻³) in acetonitrile solution. (A) Absorbance at 555 nm in the presence of 5.2×10^{-5} mol dm⁻³ various cations and (B) comparison of the absorbance at 555 nm in the presence of Pb²⁺ only with those in the presence of Pb²⁺ and other cations. The concentrations of the cations are kept to be 5.2×10^{-5} mol dm⁻³.

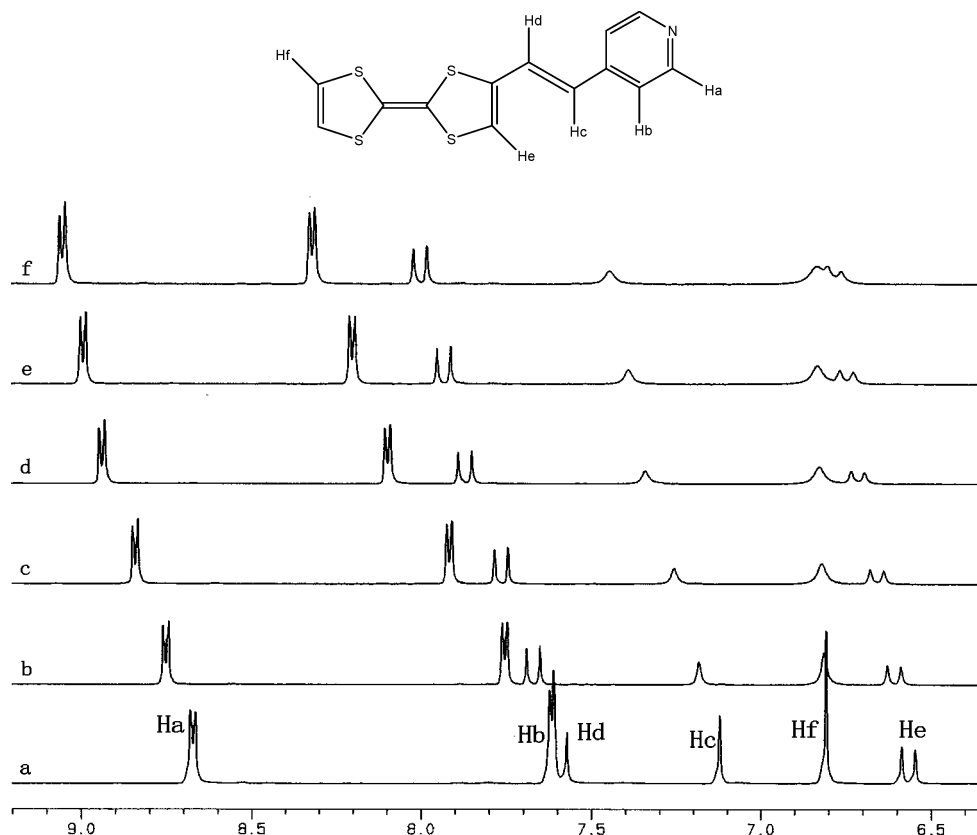


FIGURE 5. ¹H NMR spectra of **1a** (2.1×10^{-3} mol dm⁻³) in CD₃COCD₃ as a function of Pb²⁺ concentration. [Pb²⁺]: (a) 0; (b) 3.2×10^{-4} mol dm⁻³; (c) 7.4×10^{-4} mol dm⁻³; (d) 12.7×10^{-4} mol dm⁻³; (e) 15.8×10^{-4} mol dm⁻³; and (f) 21.0×10^{-4} mol dm⁻³.

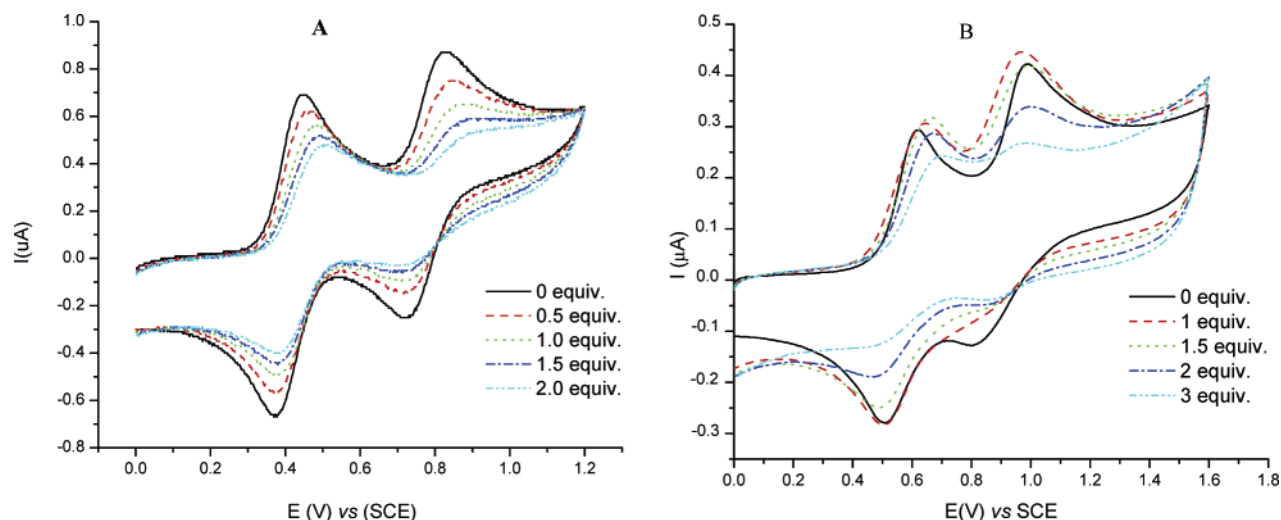
generally remains unchanged because the metal cation has been released when the TTF unit is oxidized to its dication state. The Pb²⁺-induced alteration of E_{ox}^2 in **1a** and **2a** provides indirect evidence for the binding site on the pyridyl group rather than on the TTF moiety. The metal cation and the TTF dication are far separated.

As a result, the repulsive electrostatic interaction between them is not predominant. It should be emphasized that alkali and alkaline earth metal cations do not cause any change in the oxidative potentials of the TTF moiety in **1a** and **2a**. Compounds **1a** and **2a** specifically respond to Pb²⁺.

TABLE 1. Oxidative Potentials of **1a**, **2a**, **1b**, **2b**, and Parent TTF in the Presence and Absence of Pb²⁺^a

	TTF (mV)	1a (mV)	1b (mV)	2a (mV)	2b (mV)	1a .Pb ²⁺	2a .Pb ²⁺
E^1_{ox}	382 ^b	440 ^b	412 ^b	578 ^b	465 ^b	510 ^c	695 ^d
E^2_{ox}	768 ^b	805 ^b	796 ^b	945 ^b	822 ^b	885 ^c	980 ^d

^a The data are given in mV vs a saturated calomel electrode in acetonitrile and ⁿBu₄NPF₆ (0.1 mol dm⁻³) as the supporting electrolyte. ^b In the absence of Pb²⁺. ^c In the presence of 2 equiv of Pb²⁺. ^d In the presence of 3 equiv of Pb²⁺.

**FIGURE 6.** Cyclic voltammograms of **1a** (2.9×10^{-3} mol dm⁻³) (A) and **2a** (1.8×10^{-4} mol dm⁻³) (B) as a function of Pb²⁺ concentration, recorded in a mixture of CH₃CN with ⁿBu₄NPF₆ (0.1 mol dm⁻³) as the supporting electrolyte.

Conclusion

Two TTF-pyridyl derivatives **1a** and **2a** along with the TTF-phenyl compounds **1b** and **2b** have been synthesized. In these compounds, the TTF moiety and pyridyl group or phenyl group are bridged via a double bond, which was designed to optimize the communication between the TTF unit and the pyridyl or phenyl group. The interaction between pyridyl group and Pb²⁺ enhances the electron-accepting ability of the pyridyl group. Addition of Pb²⁺ to the solution of **1a** and **2a** results in the color change of the solution from yellow to deep purple, the downfield shift of the chemical shifts of the resonances associated with the protons in ¹H NMR, and the shift of the oxidation potentials E^1_{ox} and E^2_{ox} to more positive potentials. These dramatic changes are specific for Pb²⁺. Therefore, **1a** and **2a** can be utilized as chemosensors for the detection of Pb²⁺ in the presence of other metal ions.

Experimental Procedures

Materials and Reagents. 4-Monoformyl-TTF and 4,4'(5')-bisformyl-TTF (Scheme 1), as well as 4-picolyltriphenylphosphonium chloride hydrochloride and benzyltriphenylphosphonium chloride, were prepared according to literature methods.^{17–19} Acetonitrile and tetrahydrofuran (THF) were distilled after refluxing for 3 h in the presence of P₂O₅ or sodium. Other reagents were of analytical grade and were used as received.

4-(4-Pyridineethenyl)tetrathiafulvalene (1a). CH₃ONa (242 mg, 2.2 equiv) was added to a stirred suspension of 4-picolyltriphenylphosphonium chloride hydrochloride (470 mg, 1.1 equiv) in fresh distilled anhydrous THF (20 mL) at 30 °C under an argon atmosphere. After stirring for 1 h, a solution of 4-monoformyl-tetrathiafulvalene (**3**) (232 mg, 1 mmol) in fresh distilled anhydrous THF (10 mL) was added dropwise.

After the solution was stirred for 24 h, the solid was isolated by filtration. Evaporation of the solvent from the filtrate, then chromatography on silica gel by using diethyl ether as eluent, afforded the crude product. Further recrystallization of the crude product from diethyl ether/ethyl acetate (5:1, v/v) produced **1a** as a red solid with a 60% yield; mp 133–134 °C; IR (KBr, cm⁻¹): 2922, 2853, 2046, 1632 (s); MS (EI): m/z = 307 (M⁺); ¹H NMR (CD₃COCD₃, δ ppm): 6.57 (d, J = 16 Hz, 1 H), 6.81 (s, 2 H), 7.12 (s, 1 H), 7.59 ~ 7.62 (m, 3 H), 8.67 (d, J = 8 Hz, 2 H); ¹³C NMR (CDCl₃, δ ppm): 119.0, 120.7, 122.4, 124.5, 128.4, 128.6, 131.9, 132.0, 132.1, 149.9; Anal. Calcd for C₁₃H₉NS₄·0.25C₂H₅OC₂H₅: C 51.61, H 3.53, N 4.30; found: C 51.44, H 3.28, N 4.14.

4-Styryltetrathiafulvalene (1b). Compound **1b** was synthesized by the procedure similar to that for **1a**, except that benzyltriphenylphosphonium chloride (427 mg, 1.1 equiv) was used in place of 4-picolyltriphenylphosphonium chloride hydrochloride. This product was obtained as a red solid after separation by chromatography on silica gel (dichloromethane as eluent) followed by recrystallization from petroleum ether. Yield: 46%. mp 135–137 °C. IR (KBr, cm⁻¹): 2961, 2923, 2062, 1633 (s); MS (EI): m/z = 306 (M⁺); ¹H NMR (CD₃CN, δ ppm): 6.57 (d, J = 16 Hz, 1 H), 6.64 (s, 2 H), 6.77 (s, 1 H), 7.23 (d, J = 16 Hz, 1 H), 7.42 (t, J = 8 Hz, 1 H), 7.50 (t, J = 8 Hz, 2 H), 7.62 (d, J = 7.2 Hz, 2 H); ¹³C NMR (CDCl₃, δ ppm): 118.4, 119.0, 120.3, 126.5, 128.1, 128.8, 132.0, 136.0, 136.4; Anal. Calcd for C₁₄H₁₀S₄·0.25H₂O: C 54.11, H 3.38; found: C 54.00, H 3.43.

4,4'(5')-[Bis-(4-pyridineethenyl)]tetrathiafulvalene (2a). CH₃ONa (484 mg, 4.4 equiv) was added to a stirred suspension of 4-picolyltriphenylphosphonium chloride hydrochloride (940 mg, 2.2 equiv) in fresh distilled anhydrous THF (50 mL) at 30 °C under argon. Stirring was continued for 1 h. Then, a solution of 4,4'(5')-bisformyl-tetrathiafulvalene (**4**) (262 mg, 1 mmol) in fresh distilled anhydrous THF (20 mL) was added. After a further 24 h stirring, the solid was isolated by filtration. Evaporation of the solvent from the filtrate, then chromatography on silica gel by using acetone as an eluent, gave **2a** as its two isomers: 4,4' -[bis-(4-pyridineethenyl)]tetrathiaful-

valene and 4,5'-[bis-(4-pyridineethenyl)]tetrathiafulvalene. Further recrystallization from acetone produced **2a** as a dark red solid with yield 29%; mp > 230 °C decomposition. IR (KBr, cm^{-1}): 2961, 2922, 2853, 2046, 1632 (s); MS (FAB): $m/z = 410$ (M^+); ^1H NMR ($\text{DMSO}-d_6$, δ ppm): 6.38 (d, $J = 16$ Hz, 2 H), 7.10 (s, 2 H), 7.46 (d, 2 H), 7.48 (d, 4 H), 8.48 (d, $J = 8$ Hz, 4 H); ^{13}C NMR (CDCl_3 , δ ppm): 120.7, 121.8, 124.2, 129.1, 135.1, 143.7, 149.9, 150.2; Anal. Calcd For $\text{C}_{20}\text{H}_{14}\text{N}_2\text{S}_4$: C 58.50, H 3.44, N 6.82; found: C 58.23, H 3.51, N 6.60.

4,4'(5')-Bis-styryltetrathiafulvalene (2b). The procedure for the synthesis of **2b** was similar to that for **2a**, except that benzyltriphenylphosphonium chloride (855 mg, 2.2 equiv) was used in place of 4-picolyltriphenylphosphonium chloride hydrochloride. Compound **2b** in two isomers (4,4'-bis-styryltetrathiafulvalene and 4,5'-bis-styryltetrathiafulvalene) was obtained as a red solid after separation by chromatography on silica gel (dichloromethane as eluent) followed by recrystallization from dichloromethane/petroleum ether (2:5 v/v). Yield: 40%. mp > 192 °C decomposition. IR (KBr, cm^{-1}): 2961, 2923, 2062, 1633 (s); MS (EI): $m/z = 408$ (M^+); ^1H NMR (CD_3COCD_3 , δ ppm): 6.46 (d, $J = 8$ Hz, 1 H), 6.50 (d, $J = 8$ Hz, 1 H), 6.86 (s, 2 H), 7.23 (d, $J = 16$ Hz, 2 H), 7.28–7.32 (m, 4 H), 7.36–7.40 (m, 4 H), 7.58 (d, $J = 8$ Hz, 4 H); ^{13}C NMR (CDCl_3 , δ ppm): 118.2, 118.3, 120.3, 126.5, 128.2, 128.8, 132.2, 135.9, 136.3. Anal. Calcd for $\text{C}_{22}\text{H}_{14}\text{S}_4$: C 64.70, H 3.92; found: C 64.50, H 3.93.

Binding Constant Determination. The absorption spectral titration for the determination of binding constants was performed at 298 K. The supporting electrolyte (0.1 mol dm^{-3} tetrabutylammonium hexafluorophosphate) was added to maintain a constant ionic strength of the sample solution. The ion-

binding constants (K_s) were calculated from the following equation:²⁰

$$A = A_0 + ((A_{\text{lim}} - A_0)/2C_0)(C_0 + [\text{M}] + 1/K_s - ((C_0 + [\text{M}] + 1/K_s)^2 - 4C_0[\text{M}])^{0.5}) \quad (1)$$

where A and A_0 are the absorbance for **1a** (at 555 nm) or **2a** (at 540 nm) in the presence and absence of metal ion, respectively; C_0 is half of the concentration of **1a** or the concentration of **2a**; $[\text{M}]$ is the concentration of the metal ion; and A_{lim} is the limiting value of the absorbance in the presence of excess metal ion.

Acknowledgment. We thank the National Science Foundation of China (Grants 20125207, 20333080, and 20332040) and the Ministry of Science and Technology of China (Grants G2000078104, 2003CB716802, and 2004CB719903) for financial support. We also thank the editor and the anonymous reviewers for valuable comments and suggestions.

Supporting Information Available: Physical measurements and instrumentation, UV–vis titration spectrum of **2a** in acetone with Pb^{2+} , UV–vis titration spectrum of **1a** in the presence of Ag^+ with Pb^{2+} in acetonitrile, and CV titration spectrum of reference compounds **1b** and **2b** with Pb^{2+} . This material is available free of charge via the Internet at <http://pubs.acs.org>.

JO051091R